Experimental investigation of electron transport properties of (Mo/Au)/$Al_{0.26}Ga_{0.74}N$/GaN/Si Schottky barrier diodes

H. MOSBAHI[b], M. GASSOUMI[a,b*], I. B. I.TOMSAH[a], S. ALTHOYAIB[a], C. GAQUIERE[d], M.A. ZAIDI[a,c]
[a]*Physics Department, Collage of Science, Qassim University, P.O. 6644, 51452 Buryadh, Arabie Saoudite*
[b]*Université Monastir, Monastir 5000, Tunisia*
[c] *Collage of Azolfi, Azolfi 11932, Saudi Arabia*
[d] *Université des Sciences et Technologies de Lille, Institut d'Electronique et de Microélectronique et de Nanotechnologie (IEMN), France.*

AlGaN/GaN/Si Schottky barrier diodes have been investigated using the current-voltage measurements in the wide temperature range of 125 – 500K. Measurements were performed an increase in barrier height and a decrease in the ideality factor with increasing temperature. This is attribued to barrier inhomogeneities by assuming a Gaussian distribution of barrier heights. It is also found that the values of series resistance obtained from Cheung's method strongly depend on temperature and decrease with increasing temperature. As is shown, the temperature-dependent current-voltage characteristics of the Schottky barrier diodes have been explained by invoking a double Gaussian distribution at the metal/semiconductor interface. Finally, the thermionic field emission is considered as the phenomena responsible for the excess currents observed in Schottky barriers.

(Received April 15, 2015; accepted May 7, 2015)

Keywords: AlGaN/GaN/Si Schottky diode, Current-Voltage(I-V) characteristics, Barrier Inhomogeneities(BI), Thermionic Field Emission (TFE)

1. Related works

In recent decades, AlGaN/GaN high electron mobility transistors (HEMTs) have generated much interest for high-power and high frequency applications [1, 2]. Gallium nitride is an ideal candidate for these applications due to its wide band gaps, high saturation velocity, large breakdown bias voltages, strong spontaneous and piezoelectric polarisation fields, ability to form high-quality heterostructures as well as an efficient carrier transport. A two-dimensional electron gas (2DEG) can occur at the AlGaN/GaN heterointerface with a comparatively high density, as a result from this last feature. A considerable advance is achieved in this research field.

Defects and impurities, however, are inevitable and can therefore behave as trapping centers, leading to a limitation of the devices' performance. To overcome inconveniences and limitations of the trapping effects, surface passivation is recommended as a technological solution for AlGaN/GaN transistors. Passivation is a more method to reduce electron traps [3] and increase in the drain-current as well as in cut-off frequency and i microwave output power [4,5]. Passivation with N2O pretreatment improves the electron transport and reduces the trapping effects [6].

The mechanism of leakage currents through GaN and AlGaN Schottky interfaces is treated with temperature dependence of the current-voltage (I-V-T) characteristics allows the identification of the various conduction mechanism modes through the metal/GaN interface and the study of different effects, such as surface states density and barrier inhomogeneities [7,8]. Duo to technological importance of Schottky barrier diodes, many theoretical and experimental investigations of the current flow mechanism in Schottky barriers have been reported in the literature [7-10]. Several results were obtained for the AlGaN/GaN heterostructures studies. This has been elucidated by a well-clear increase in the ideality factor and decrease in the barrier height with decreasing temperature [11,12]. To explain these features, it has been assumed that the integration of the concept of barrier inhomogeneities and the introduction of Gaussian distribution function with a mean and standard deviation for the description [13,14]. While the anomalies were explained through thermionic emmision mechanism supposing that there is existence of Gaussian distributions of barrier heights to explain the large leakage currents in GaN and AlGaN Schottky barriers [15]. Well as the increase in the ideality factor at low temperature may be due to generation-recombination centers [16]. Compared to Ref [7], the temperature dependence of ideality factor and barrier height is explained on the basis of thermionic emission mechanism supposing the presence of double Gaussian distribution of barrierheights. On the other hand, the series resistance increases with increasing temperature [17]. They reported to the lack of free charge carriers, particularly, at low temperatures [18].

In the present work reports on a study of AlGaN/GaN/Si Schottky barrier diodes using current-voltage characteristics. We have also investigated the ideality factor, barrier height, series resistance and Richardson's constant. An attempt to correlate all of the results has been made in order to explain by the thermionic emission mechanism by assuming the existence of double Gaussian distributions of barrier heights and by quantum mechanical tunneling including the thermionic field emission.

2. Experimental details

The AlGaN/GaN HEMTs under investigation are grown on silicon (111) substrate by using molecular beam epitaxy (MBE). The active layers consist in a 500 nm thick of undoped AlN/AlGaN buffer, a 1.8 µm undoped GaN channel, a 23 nm thick ofundoped $Al_{0.26}GaN_{0.74}N$ barrier and a 1 nm n^+-GaN cap layer. The device processing is made following conventional HEMT fabrication steps. The ohmic contact pads are patterned using e-beam lithography. Hereafter, the metallization by means of evaporated 12/200/40/100 nm Ti/Al/Ni/Au is deposited at 900°C during 30s. The Schottky gate is realized using 100/150 nm Mo/Au layers. On the other hand, the AlGaN/GaN HEMTs are passivated by 100/50 nm SiO_2/SiN with N_2O pretreatment. The current-voltage characteristics of the device were measured in the temperature range of 125-500 K by steps of 25 K using keithley source measuring unit 4200. The device temperature was controlled with an accuracy of ± 2 K by using temperature controller PID.

3 Results and discussion

The current-voltage characteristics of an ideal Schottky barrier diodes (SBD) are given by thermionic emission (TE) theory [19]. For bias voltage $V > \frac{3KT}{q}$, the conventional diode equation can be expressed as :

$$I = I_0 \exp\left(\frac{qV}{\eta KT}\right) \tag{1}$$

with :

$$I_0 = A A^* T^2 \exp\left(-\frac{q\Phi_{ap}}{KT}\right) \tag{2}$$

where Φ_{ap} is the zero bias apparent barrier height (BH), q is the electron charge, T is the absolute temperature, K is the Boltzmann constant, A^* is the effective Richardson constant ($A^* = 26.4$ A/cm^{2}K^2 for GaN) and A is the diode area. The apparent barrier height were determined using :

$$\Phi_{ap} = \frac{KT}{q} \mathrm{Ln}\left(\frac{AA^*T^2}{I_0}\right) \tag{3}$$

where I_0, is the saturation current, is obtained by extrapolating the linear region of the curve LnI vesus V to zero applied voltage. For the ideality factor, it can be evaluated from the slope of the LnI-V plots using the relation

$$\eta = \frac{q}{KT}\left(\frac{dV}{d(\mathrm{LnI})}\right) \tag{4}$$

Fig.1 shows the forward and reverse bias current-voltage characteristics of (Mo/Au)/AlGaN/GaN/Si Schottky diode in the temperature range 125-500 K. It is seen that the leakage current increases with an increase in temperature and the values are in the range of 4.125×10^{-6} A (at 125 K) to 4.613×10^{-5} A (at 500 K) at -1V.

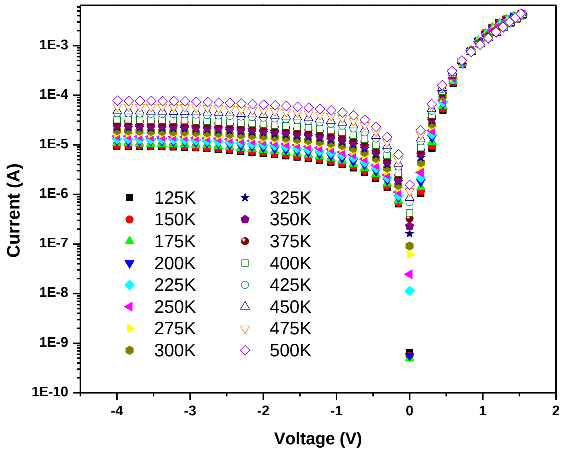

Fig.1 Experimental forward and reverse current-voltage of the (Mo/Au)/AlGaN/GaN/Si Schottky diode for different temperatures.

In Fig.2, we report the Schottky barrier height as well as the ideality factor versus temperature. The values of SBH (Φ_{ap}) and 5 vary from 0.23 eV and 2.02 at 125 K to 0.87 eV and 1.39 at 500 K respectively. The SBH decreases and the ideality factor increases with decrease in temperature. As an attempt of explanation, the decreasing of SBH (Φ_{ap}) and the increase in factor ideality at low temperature are possibly caused by a non-uniformity of the interfacial charges, inhomogeneities in thicknesses and alloy compositions of the epilayers, the presence of a thin insulating layer between the metal and the semiconductor or the surface states [20,21]. It is worth to notice that these imperfections can introduce inhomogeneities into the transport current. Therefore, the transport of current across the metal/semiconductor heterointerface is a temperature-activated process [22-24]. This can explain very well why the electron transport at low temperature is dominated by the current throught the patches of lower Schottky barrier height, leading to a larger ideality factor. In a model developed by Werner [22], proposed that such dependence is originated by Schottky barrier inhomogeneity which may be caused several interface quality which depends on various factors such as the surface treatment, the metal and the deposition process and the surface defects density [22,25,26]. Furthermore, the surface defects or local enhancement of electric field can also give a lateral reduction in the Schottky barrier height. This allows to inhomogeneities in the transport current.

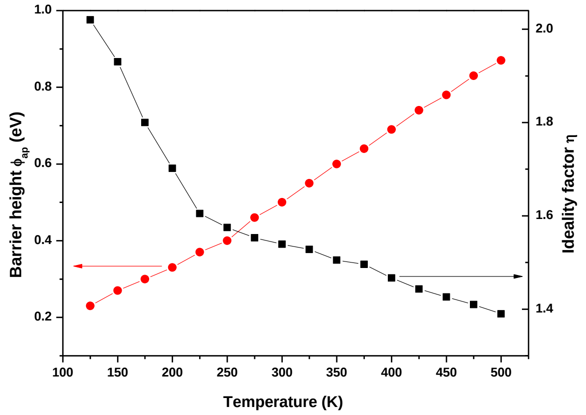

Fig.2 Temperature-dependence of the apparent barrier height and ideality factor

The series resistance is an important parameter of Schottky diodes. The series resistance can be evaluated from the forward bias current-voltage data using the methode developed by Cheung and cheung [27]. It is given according to :

$$\frac{dV}{d(LnI)} = I\,R_s + \eta\left(\frac{K\,T}{q}\right) \qquad (5)$$

As shown, R_s have been obtained from the slope of the dV/dLnI versus I at a fixed temperature. Whereas **η**kt/q corresponds to the y-axis intercept. It has been found that the series resistance decreases with increasing temperature (see Fig.3). It is worth to mention that the variation of R_s with temperature may be due to the factors responsible for the increase in ideality factor and the lack of free carrier concentration at low temperature [28].

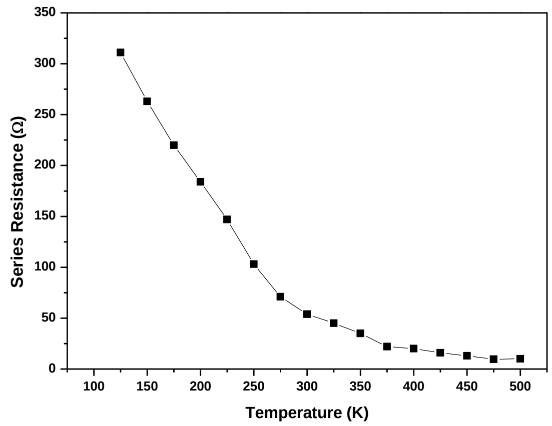

Fig.3 Temperature dependence of the series resistances

The ideality factor of the Schottky barrier diode with a distribution of low Schottky barrier height may increase with decreasing temperature [29-32]. The plot of the experimental apparent barrier height (Φ_{ap}) versus the ideality factor (5) of the (Mo/Au)/AlGaN/GaN Schottky diode is illustrated in Fig.4. It is also observed that two linear regions between Φ_{ap} and η values of the (Mo/Au)/AlGaN/GaN SBD, which can be explained by the lateral inhomogeneities of the barrier heights [31,33]. We will use Tung [30] theoretical approach that found a linear correlation between the experimental zero-bias Schottky barrier height and ideality factor. In the first region 275-500 K, the extrapolation of the experimental barrier heights versus ideality factor for η = 1 gives a homogenous barrier height of 1.85 eV. In the second region 125-275 K, the extrapolation of the experimental barrier heights versus ideality factor for η = 1 gives a homogenous barrier height of 0.56 eV. It should be noted that the decease of the zero-bias barrier height and increase of the factor ideality especially at low temperature may be caused by the barrier inhomogeneities.

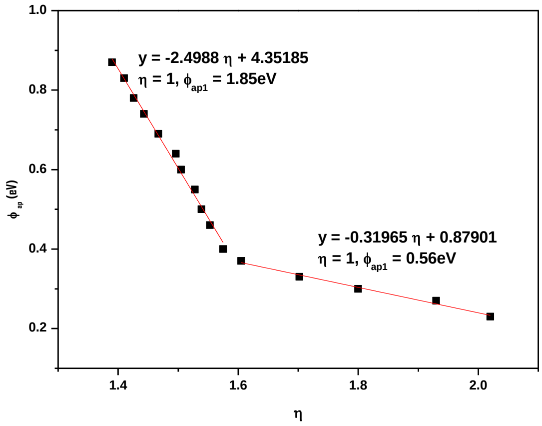

Fig.4 The apparent barrier height as a function of the ideality factor

The abnormal deviations of current-voltage characteristics of a Schottky diode has been attributed to a lateral distribution [22, 32, 34,35]. The Werner's model [22] is the most commonly used to study the Gaussian distribution of barrier heights which varies around a mean value $\overline{\Phi_{b0}}$. According to this Gaussian distribution, the expression of the barrier height is given by [36] :

$$\Phi_{ap} = \overline{\Phi_{b0}}(T=0) - \frac{q\,\sigma_0^2}{2\,K\,T} \qquad (6)$$

where σ_0 is the zero bias standard deviation of the Schottky barrier height distribution. The temperature dependence of σ_0 is usually small and can be neglected [37]. For the ideality factor 5, and based on the Gaussian distribution model, an inverse proportionality as a function of temperature can be shown by using the expression [22] :

$$\frac{1}{\eta_{ap}} - 1 = -\rho_2 + \frac{q\,\rho_3}{2\,KT} \qquad (7)$$

here η_{ap} is the apparent ideality factor, ρ_2 is the voltage coefficient of the mean SBH and ρ_3 is the voltage coefficient of the standard deviation. The Φ_{ap} and $(\eta^{-1} - 1)$ versus 1/2KT plot is given in Fig.5. According to Eq. (6), the plot of Φ_{ap} versus 1/2KT should be a straight line with y-axis intercept corresponding to the mean barrier height $\overline{\Phi}_{b0}$ and the slope give the standard deviation σ_0. The values of ρ_2 and ρ_3 obtained from the y-axis intercept and the slope of the straight lines respectively. The plot of Φ_{ap} versus 1/2KT exhibits two Gaussian distributions of barrier heights. So, we have obtained two sets of values for $\overline{\Phi}_{b0}$ and σ_0 in the temperature ranges 275-500 K and 125-275 K : in the first region are $\overline{\Phi}_{b01}$ = 1.343 eV and σ_{01} = 0.2 V, and in the second region $\overline{\Phi}_{b02}$ = 0.55 eV and σ_{02} = 0.084 V. The existence of a double Gaussian in the metal/semiconductor contacts can be assigned to the nature of the inhomogeneities themselves [37]. Similary, as can be clearly seen from Fig.5, the plot of $(\eta^{-1} - 1)$ versus 1/2KT presents two linear regions. The linear behavior of this plot demonstrates that the η is related to the voltage deformation of the Schottky barrier height. The values obtained for ρ_2 and ρ_3 are respectively : 0.18 V and -0.092 V in temperature range 275-500 K and 0.221 V and –0.006 V for temperature ranging from 125-275 K. It should be noted that the extracted values of the standard deviation and the mean barrier height indicates the presence of potentiel fluctuations at the interface and the interface inhomogeneities.

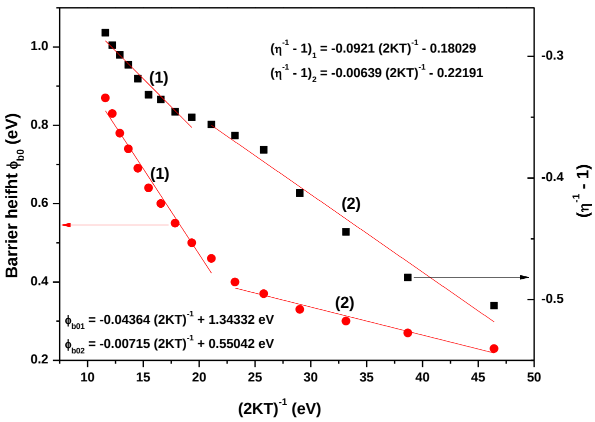

Fig.5 The apparent barrier height and ideality factor versus 1/2KT

To explain these discrepancies according to the Gaussian distribution of the barrier height, we can rewrite, Eq. (1) combined with Eq. (6), under the form :

$$\mathrm{Ln}\left(\frac{I_0}{T^2}\right) - \frac{q^2\,\sigma_0^2}{2\,K^2\,T^2} = \mathrm{Ln}\,(A\,A^*) - \frac{q\,\overline{\Phi}_{b0}}{KT} \qquad (8)$$

Fig. 6 depicts the plot of $\left[\mathrm{Ln}\left(\frac{I_0}{T^2}\right) - \frac{q^2\,\sigma_0^2}{2\,K^2\,T^2}\right]$ versus 1000/T. Liner fitting of the curve gives the Richardson constant A^* and the mean barrier height $\overline{\Phi}_{b0}$. This plot should give a straight line with slope directly yielding the $\overline{\Phi}_{b0}$ and the intercept (Ln AA^*) at the ordinate determining A^* for a given diode area A. The relevant values are 0.877 eV and 27.65 $Acm^{-2}K^{-2}$ in the temperature 275-500 K and 1.02 eV and 11.37 $Acm^{-2}K^{-2}$ as temperature varies between 125 and 275 K. It should be noted that the values of the Richardson constant are close to the theoretical value 26.4 $Acm^{-2}K^{-2}$ for n-GaN [38]. The experimental Richardson constant has different values for the different temperature range is most likely due to the inhomogeneity in the barrier.

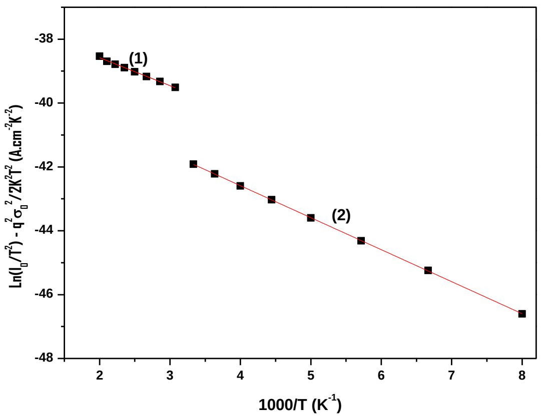

Fig.6 Modified Richardson plot $\left[\mathrm{Ln}\left(\frac{I_0}{T^2}\right) - \frac{q^2\,\sigma_0^2}{2\,K^2\,T^2}\right]$ *versus 1000/T*

The thermionic field emission (TFE) is considered as the phenomena responsible for the excess currents observed in the Schottky barrier. If the current transport is monitored by the TFE theory, the relation between the current and voltage can be expressed as [19] :

$$I = I_0 \exp\left(\frac{q\,V}{E_0}\right) \qquad (9)$$

with :

$$E_0 = E_{00} \coth\left(\frac{q\,E_{00}}{KT}\right) = \frac{\eta\,KT}{q} \qquad (10)$$

where E_{00} is the characteristic tunneling energy that is related to the tunnel effect transmission probability and is given by :

$$E_{00} = \frac{h}{4\pi}\left(\frac{N_d}{\varepsilon_s m_e^*}\right)^{1/2} \quad (11)$$

where h is the Plank's constant, ε_s is the dielectric constant, m_e^* is the electron effective mass and N_d is the carrier concentration. E_{00} is found to be about 0.0076 eV. When considered the bias coefficient of the barrier height (β), Eq. (10) can be written as [39,40] :

$$\eta_{tun} = \frac{E_0}{KT(1-\beta)} \quad (12)$$

Fig.7 shows the ideality factor as a function of temperature for the case when the current throught the Schottky junction is dominated by the TFE. A best fit of the ideality factor is achieved for E_{00} = 21.8 meV. Whereas β = 0, it is found that there is a substantial consistency between the experimental and theoretical characteristics. The possible origin of the high characterisctics energy values E_{00} is connected with the transmission probability, characterizing the electric field at the surface of the semiconductor to a given applied bias [7,30]. Consequently, any mechanism which enhances the state density or the electric field at the semiconductor will increase the thermionic field emission well as E_{00}. Given that the improvement of the transmission probability may be due to local improvement of electric field, it can also enable a local reduction of the barrier height [41,42]. In our case, we awarded the dominance of TFE can be linked to the Gaussian distribution of the barrier height.

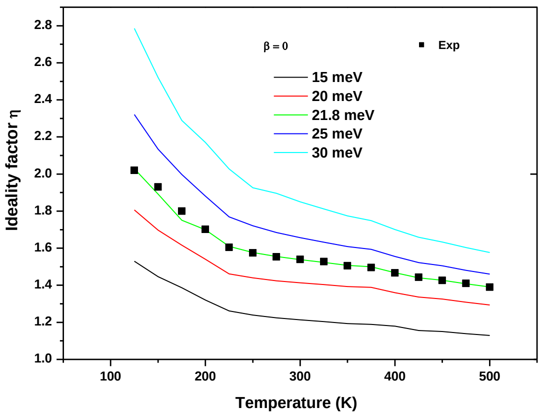

Fig.7 Theoretical temperature dependence of the ideality factor.

4. Summary

In the present work, we have investigated the electrical transport characteristics of (Mo/Au)/AlGaN/GaN Schottky diode. The electrical behavior of the transistor devices is characterized by using I-V measurements. As has been shown, the ideality factors increase and the decreasing trend of the barrier height with a decrease in temperature. The temperature dependence of barrier height and ideality factor has been explained based on the thermionic émission with the assumption of double Gaussian distribution of the barrier heights at the interface. In addition, we suggest that the current through the junction is also influence by the TFE mechanism.

Acknowledgement

The authors of this article would like to thank the Deanship of the Scientific Research at Qassim University, Kingdom of Saudi Arabia for their support under grant number No.2648.

References

[1] M. J. Manfra, N. Weimann, Y. Bayens, P. Roux, D. M. Tennant, Electron Lett. **39,** 694 (2003).
[2] V. Kumar, A. Kuliev, R. Schwindt, M. Muir, G. Simin, J. Yang, M. A. Khan, I. Adesida, Solid-State Electron. **47,** 1577 (2003).
[3] M. J. Tadjer, T. J Anderson, K. D. Hobart, M. A. Mastro, J. K. Hite, J. D. Caldwell, Y. N. Picaed, F.J.Kub, C.R.Eddy J.r., J. Electron Mater. **39,** 2452 (2010).
[4] J. Bernat, P. Javorka, M. Marso, P. Kordos, Appl.Phys.Lett. **73,** 5455 (2003).
[5] M. Gassoumi, H. Mosbahi, A. Soltani, V. S-Avramovic, M. A. Zaidi, C. Gaquiere, H. Maaref, Mat.Sci.in Semiconductor Processing. **16,** 1775 (2013).
[6] H. Mosbahi, M. Gassoumi, I. Saidi, H. Mejri, C. Gaquiere, M. A. Zaidi, H. Maaref, Current Applied Physics. **13,** 1359 (2013).
[7] M. S. P. Reddy, A. A. Kumar, V. R. Reddy, Thin Solid Films. **519,** 3844 (2011).
[8] S. Dogan, S. Duman, B. Gürbulak, S. Tüzemen, H. Morkoç, PhysicaE. **41,** 646 (2009).
[9] V. R. Reddy, N. N. K. Reddy, Superlattices and Microstructures. **52,** 484 (2012).
[10] K. Hayashi, Y. Yamaguchi, T. Oishi, H. Otsuka, K. Yamanaka, M. Nakayama, Y. Miyamoto, Jap. J. Appl.Phys. **52,** 04CF12 (2013).
[11] M. R. H. Khan, T. Detchprohm, P. Hacke, K. Hiramatsu, N. Sawaki, J. Phys. D : Appl. Phys. **28**, 1169 (1995).
[12] E. V. Kalinina, N. I. Kuznetsov, V. A. Dmitriev, K. G. Irvine, C. H. Carter, J. Elect. Mater. **25,** 831 (1996).
[13] S. Duman, B. Gurbulak, A. Turut, Appl. Surf. Sci. **253,** 3899 (2007).
[14] A. F. Ozdemir, A. Turut, A. Kokce, Semicond. Sci.Technol. **21,** 298 (2006).
[15] H. Hasegawa, M. Akazawa, Appl.Surf.Sci. **254**, 3653 (2008).
[16] Z. Benamara, B. Akkal, A. Talbi, B. Gruzza, Mater.Sci.Eng.C. **26**, 519 (2006).

[17] Z. Tekeli, S. Altindal, M. Cakmak, S. Ozcelik, D. Caliskan, E. Ozbay, J. Appl. Phys. **102,** 054510 (2007).
[18] E. Arslan, Y. Safak, S. Altindal, O. Kelekci, E. Ozbay, J.Non-Cryst.Solids. **356,** 1006 (2010).
[19] E. H. Rhoderiek, R. H. Williams, Metal-Semiconductor Contacts, 2nd ed., Clarendon, Oxford (1988).
[20] Y.Nakano, T.Jimbo, Appl.Phys.Lett. **80**, 4756 (2002).
[21] C.Bal, C.Krug, G.Lucovsky, J.Vac.Sci.Technol.A. **22**, 2379 (2004).
[22] J. H. Werner, H. H. Guttler, J. Appl. Phys. **69,** 1522 (1991).
[23] A. Gumus, A. Turut, N. Yalcin, J.Appl.Phys. **91,** 245 (2002).
[24] S. Karatas, S. Altindal, A. Turut, A. Ozmen, Appl. Surf. Sci. **217**, 250 (2003).
[25] Y. Zhou, D. Wang, C. Ahyi, C. C. Tin, J. Williams, M. Park, N. M. Wiliams, A. Hanser, E. A. Preble, J. Appl. Phys. **101**, 024506 (2007).
[26] S. Arulkumaran, T. Egawa, H. Ishikawa, M. Umeno, T. Jimbo, IEEE Trans.Elec.Dev. **48**, 573 (2001).
[27] S.K.Cheung, N.W.Cheung, Appl.Phys.Lett. **49,** 85 (1986).
[28] S.Chand, J.Kumar, Appl.Phys.A. **63**, 171 (1996).
[29] J. P. Sullivan, R. T. Tung, M. R. Pinto, W. R. Graham, J.Appl.Phys. **70**, 7403 (1991).
[30] R.T.Tung, Appl.Rev.B. **45**, 13509 (1992).
[31] R. F. Schmisdorf, T. U. Kampen, W. Monch, Surf.Sci. **324**, 249. (1995)
[32] S.Chand, J.Kumar, J.Appl.Phys. 80 (1996) 288.
[33] S. Zeyrek, S. Atindal, H. Yuzer, M. M. Bulbul, Appl. Surf. Sci. **252**, 2999 (2006).
[34] J. Osvald, Z. J. Horvath, Appl.Surf.Sci. **234**, 349 (2004).
[35] S. Chand, S. Bala, Appl.Surf.Sci. **252**, 358 (2005).
[36] S. Zhu, R. L. Van Meirhaeghe, C. Detavernier, F. Cardon, G. P. Ru, X. P. Qu, B. Z. Li, Solid State Electron. **44**, 663 (2000).
[37] S. Chand, J. Kumar, Semicond.Sci.Technol. **11**, 1203 (1996).
[38] X. J. Wang, L. He, J. Electron Mater. **27**, 1272 (1998).
[39] S. Y. Han, K. J. Choi, J. L. Lee, J. K. Mun, M. Park, H.Kim, J.Vac.Sci.Technol.B. **21**, 2133 (2003).
[40] S.H.Huang, Y.Tian, F.Lu, Appl.Surf.Sci. **234,** 362 (2004).
[41] Z. J. Horvath, V. Rakovics, B. Szentpali, S. Puspoki, K.Zansky, Vaccuum. **71**, 113 (2003).
[42] E.Ayyildiz, H.Cetin, Z.J.Horvath, Appl.Surf.Sci. **252,** 1153 (2005).

*Corresponding author : malek.gassoumi@gmail.com